

Divalent-to-trivalent transition of Sm in SmS: Implications for the high-pressure magnetically ordered state

E. Annese,¹ A. Barla,^{2,*} C. Dallera,³ G. Lapertot,² J-P. Sanchez,² and G. Vankó⁴

¹*INFN-Dipartimento di Fisica, Università degli Studi di Modena e Reggio Emilia, via Campi 213/A, I-41100 Modena, Italy*

²*Département de Recherche Fondamentale sur la Matière Condensée, CEA Grenoble, 17 rue des Martyrs, F-38054 Grenoble Cedex 9, France*

³*INFN-Dipartimento di Fisica, Politecnico di Milano, piazza Leonardo da Vinci 32, I-20133 Milano, Italy*

⁴*European Synchrotron Radiation Facility, Boîte Postale 220, F-38043 Grenoble Cédex, France*

(Received 19 December 2005; revised manuscript received 8 March 2006; published 28 April 2006)

We present a resonant x-ray emission study of the pressure-induced valence transition of SmS. Spectra excited at the L_3 absorption edge of Sm ions were recorded at applied pressures ranging from 1 to 18 GPa, at room temperature. Thanks to its extreme sensitivity to the electronic configuration, resonant inelastic x-ray emission is well suited to follow precisely the small valence changes in the high pressure region. The Sm valence is found to increase from 2.7 at 1 GPa to 3 at 18 GPa, and the trivalent state is reached at $p_c \sim 13$ GPa. Our results imply that the transition to the trivalent state at p_c is not accompanied by any detectable change of the magnetic properties, as inferred from the nuclear forward scattering measurements, with respect to those of the intermediate valent state ($p > 2$ GPa).

DOI: [10.1103/PhysRevB.73.140409](https://doi.org/10.1103/PhysRevB.73.140409)

PACS number(s): 75.30.Mb, 78.70.Ck, 71.27.+a, 71.28.+d

SmS has been extensively studied in the last three decades because of its isostructural first-order electronic phase transition (“black-gold” transition), that occurs at the very low pressure $p_{B-G}=0.65$ GPa at room temperature.^{1,2} At ambient pressure SmS is a nonmagnetic semiconductor with NaCl-type structure and the Sm ions have a divalent configuration ($4f^6$). In the semiconducting phase the $4f$ levels are close to the Fermi level, lying between the valence and $5d$ conduction band split by the crystal field into $5d(t_{2g})$ and $5d(e_g)$ subbands [see the inset of panel (a) in Fig. 1]. By increasing the external pressure and hence reducing the lattice constant, the $5d(t_{2g})$ and $5d(e_g)$ splitting increases [see the inset of panel (b) in Fig. 1]. At p_{B-G} the $5d(e_g)$ band overlaps with the $4f$ levels, the energy gap becomes zero and the transition to the metallic golden phase occurs. The occupancy of the $4f$ levels becomes noninteger because of the gradual transfer of a $4f$ electron into a $5d$ state, giving rise to an intermediate valence state. The first evidence of the pressure-induced semiconductor to metal transition and hints of a change of valence at p_{B-G} at room temperature date from the beginning of the 1970s, when an abrupt decrease of resistivity and the lattice constant were observed.² Further effects related to the electronic transition under pressure, such as the color change from black to golden,¹ a first-order transition of the magnetic susceptibility³ and phonon anomalies due to the large difference in ionic radii associated with the two valence states⁴ were noted throughout time at room temperature. In addition, resistivity measurements performed on SmS in the golden phase have revealed the presence of a semiconducting ground state [a small gap opens at low temperatures (some degrees K)] below 2 GPa, above which the ground state becomes metallic.⁵ Just above p_{B-G} , the valence of Sm was determined from spectroscopic, Mössbauer, and lattice constant measurements, which gave a valence value of 2.6, 2.65–2.7, or 2.8, respectively.^{3,6,7} In particular, x-ray absorption (XAS) measurements, performed by Röhler *et al.*⁶ at the Sm L_3 edge at room temperature in the pressure range from

0.1 MPa to 7.2 GPa, gave a non-linear dependence of the valence upon pressure with an inflection point at 2 GPa.

One open question concerning the behavior of SmS under pressure is whether Sm becomes completely trivalent above 7.2 GPa. This is interesting in order to find out any interplay among valence, conductivity, and magnetism in this compound. From the large pressure derivative of the bulk modulus found in the metallic phase at room temperature it was suggested by Keller *et al.*⁸ that a normal trivalent behavior should be observed at around 10 GPa. For trivalent Sm one expects a magnetic ground state, which was, however, not observed in susceptibility measurements performed in the golden phase just above p_{B-G} (up to 0.8 GPa).³ On the other hand, band structure calculations predict a nonvanishing magnetic moment in the metallic intermediate valent phase.⁹ A first-order transition from a nonmagnetic to a magnetically ordered state with magnetic moment $\mu=0.5\mu_B$ above 2 GPa was recently observed by ¹⁴⁹Sm nuclear forward scattering of synchrotron radiation and specific heat measurements.^{10–12} The magnetic state of SmS was found to correspond to that of a stable trivalent compound, with ordering temperature T_m increasing from 15 K at 2 GPa to 24 K at 8 GPa. These recent results called for an accurate determination of the Sm valence in the (p, T) space and motivated us to reinvestigate the problem over a wider pressure range than done in previous spectroscopic experiments,^{3,6} by means of resonant x-ray emission spectroscopy (RXES).

RXES has been shown to be a very effective tool for probing the mixed valence ground state of rare earths under pressure; e.g., in the case of intermediate valence Yb compounds, such as YbAl₂, YbS, YbAgCu₄, and YbInCu₄.^{13–16} RXES is a second order process where an incident x-ray photon with energy tuned across the absorption edge excites a core electron, and the core-excited state decays by emitting an x-ray photon of the same energy or lower energy. In the present experiment, SmS was excited at the Sm L_3 ($2p_{3/2}$) absorption edge and the $L\alpha_1$ ($3d_{5/2} \rightarrow 2p_{3/2}$) decay was re-

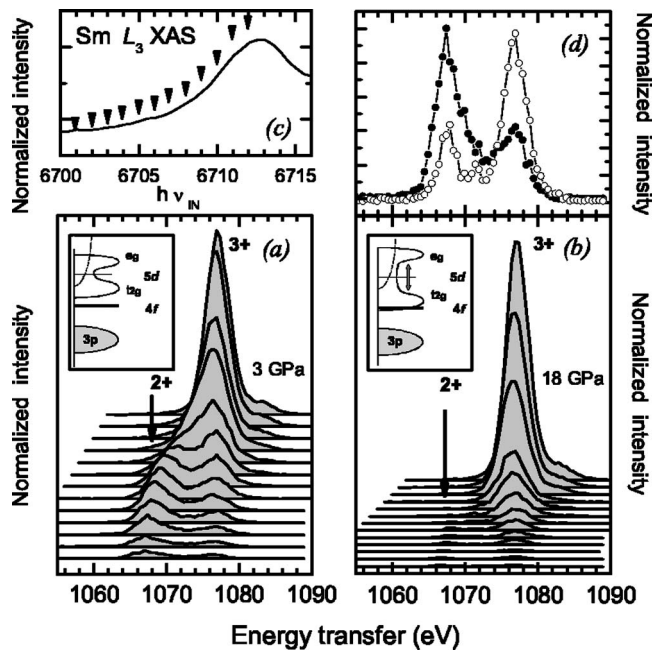


FIG. 1. (a) Full set of $L\alpha_1$ RXES spectra acquired at 3 GPa and (b) 18 GPa, for incident photon energy values from 6700 to 6712 eV. The arrows point to divalent and trivalent features in the spectra. Inset: Electronic structure of SmS in semiconducting (left-hand side) and metal (right-hand side) phase with reference to the Fermi energy: $4f$ levels lie in between the valence and $5d$ conduction band in the semiconducting phase and overlap the $5d$ states in the metal phase (as described in the text). (c) $Sm L_3$ XAS spectra measured in total fluorescence yield at 16 GPa. The arrows indicate the excitation energies for each set of $L\alpha_1$ RXES spectra. (d) $L\alpha_1$ RXES spectra measured at incident energy $h\nu_{IN}=6703$ eV for applied pressures of 3 GPa (filled circles) and 18 GPa (hollow circles).

corded. The presence of the $3d_{5/2}$ core hole in the final state gives rise to two multiplet families for Sm^{2+} and Sm^{3+} , separated by the Coulomb interaction. By evaluating the relative spectral contributions associated with Sm^{2+} and Sm^{3+} configurations, we find a valence increase from 2.7 at 1 GPa to nearly 3 at 18 GPa. In the range between 13 and 18 GPa the valence appears to approach asymptotically the +3 value, although here the uncertainty in our valence determination is comparable to the difference between the evaluated valence and 3. The Sm-monosulfide specimen used for the present study was a single crystal grown by the Bridgman method in a sealed tantalum crucible. Its dimensions were $\sim 100 \times 40 \times 50 \mu m^3$. Measurements were performed at the ESRF, Grenoble, France, on beamline ID16, equipped with a Si(111) monochromator. The emission spectrometer is of Rowland type design, and a Si(422) spherical crystal was used as analyzer for the $L\alpha_1$ ($3d_{5/2} \rightarrow 2p_{3/2}$, $h\nu_{OUT} = 5633$ eV) emission line of Sm. The overall energy resolution was 1.5 eV. The beam was focused to a size of $100 \times 45 \mu m^2 (H \times V)$ at the sample position. RXES spectra were measured at room temperature, with the sample loaded in a diamond anvil cell along with ruby chips, using high strength Be as the gasketing material. The pressure transmitting medium was Fluorinert. Pressure values were measured *in situ*

by the conventional ruby fluorescence technique. No broadening of the ruby fluorescence lines was observed at any pressure, which indicates that pressure gradients are minimal within the pressure cell and that the pressure conditions remain quasihydrostatic up to 18 GPa. The experiment was performed in radial geometry; i.e., with the incident and scattered radiation crossing the Be gasket and not the diamonds. During the experiment the ESRF ring was filled in 16 bunch mode, with a maximum ring current of 90 mA. The maximum count rate under pressure was about 4000 counts per second when exciting at the Sm^{3+} resonance.

The RXES experiment on SmS consisted in measuring the $L\alpha_1$ x-ray emission at fixed incident energies along the $Sm L_3$ absorption edge, at selected pressures in the 1–18 GPa range. In the final excited state the difference in photon energy ($h\nu_{IN} - h\nu_{OUT}$) is transferred to the system. The transferred energy is characteristic of the excited electronic configuration. Sm^{2+} and Sm^{3+} have respectively $|3d^9 4f^6 \epsilon d\rangle$ and $|3d^9 4f^5 \epsilon d\rangle$ final state configurations (where ϵd stands for an electron added above E_F to the d conduction band). The Coulomb interaction between the $3d_{5/2}$ core-hole and the $4f$ electrons splits the intermediate and final state multiplets into two families, which give rise in the emission spectrum to two peaks, at different fixed energy transfer, whose intensity is resonantly enhanced by varying $h\nu_{IN}$ across the absorption threshold.¹⁷ Panels (a) and (b) of Fig. 1 display sets of RXES spectra at 3 and 18 GPa, measured at $h\nu_{IN}$ values increasing in 1 eV steps from 6700 eV to 6712 eV along the energy region indicated on the absorption spectrum shown in panel (c). The spectra are plotted as a function of the energy $E_T = h\nu_{IN} - h\nu_{OUT}$ transferred from the photon to the solid. The divalent and trivalent features are indicated by the two arrows in Fig. 1 and are observed at fixed energy transfer values $E_T(2+) \sim 1067$ eV and $E_T(3+) \sim 1077$ eV, respectively. The asymmetric spectral shape reflects the spread of the final state multiplet. This is best seen in panel (d) of Fig. 1, where two RXES spectra at 3 and 18 GPa excited at $h\nu_{IN} = 6703$ eV (well below the absorption threshold) are shown in a zoomed view. The final state multiplet structure of samarium consists of numerous levels, as can be inferred from calculations of $M_{4,5}$ absorption.¹⁸ Each multiplet term is resonantly enhanced at a particular excitation energy. Having defined an average resonant incident energy, $h\nu_{IN}(2+)$ for Sm^{2+} and $h\nu_{IN}(3+)$ for Sm^{3+} , as the energy at which the overall intensity of their spectral contribution is highest, we find $h\nu_{IN}(2+) = 6703$ eV and $h\nu_{IN}(3+) = 6711$ eV. The evolution of the spectral shape as a function of the excitation energy allows one to separately follow and disentangle the spectral intensities of Sm^{2+} and Sm^{3+} . The intensities $I(2+)$ and $I(3+)$ at their respective resonance correspond to the weight of the divalent and trivalent samarium, by assuming that $I(2+)$ and $I(3+)$ are proportional to the number of atoms in each electronic configuration.

The valence can then be evaluated as:

$$v = 2 + \frac{I(3+)}{I(2+) + I(3+)},$$

at each pressure.

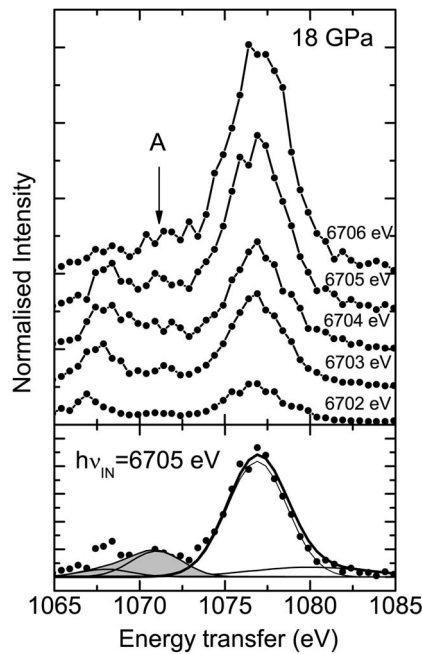


FIG. 2. Upper panel: RXES spectra recorded at incident energies ranging from 6702 to 6706 eV and at 18 GPa. The arrow indicates the position of the main component of the Sm^{3+} quadrupolar transition. Lower panel: fit of RXES spectrum at 6705 eV: trivalent dipolar contribution (thick line) and the two Gaussians used to model it; the shadowed area is the sum of two Sm^{3+} quadrupolar components. The divalent contribution (peaking at ~ 1068 eV) is obtained by subtracting from the spectra the trivalent component.

The Sm valence change against pressure is evident at a glance from Figs. 1(a) and 1(b), where the increased weight of the trivalent feature is observed, and the divalent component vanishes at the highest reached pressure of 18 GPa. In order to extract the value of the Sm valence, we decomposed the RXES spectra into the components deriving from Sm^{2+} and Sm^{3+} through a procedure following what was done for YbAl_2 and YbS in Refs. 15 and 16, and is briefly described hereafter. We started from the Sm^{3+} resonance spectrum at the highest pressure (18 GPa), where the spectral intensity derives almost completely from the $2p \rightarrow 5d$ dipolar transition of the trivalent configuration, and intensity from Sm^{2+} can be safely neglected. We modeled that peak as the sum of two Gaussians: the first centered at the energy $E_T(3+) = 1077$ eV and having a width of 3.5 eV, the second with a width of 7 eV and centered at 1080 eV. The sum of two Gaussian profiles allows a proper reproduction of the asymmetric shape of the trivalent emission line (see lower panel of Fig. 2). This profile was kept constant in the fitting of all spectra, and only its intensity was scaled to match the measured shapes. The divalent resonant profile was obtained by subtracting from the measured spectra the trivalent component. For incident energies beyond the Sm^{2+} resonance, the resonant emission from Sm^{2+} rapidly diminishes and a further component corresponding to its fluorescent emission is required to fit the RXES spectra. The fluorescent process is incoherent and gives rise to intensity that peaks at constant emitted energy. This was obtained by subtracting from the spectra the trivalent and divalent resonant components. The

fitting was optimized by scaling the trivalent component to match the high transferred energy side of the spectra with the constraints that the fluorescence component is at constant emission energy. At pressures higher than 7.7 GPa the contribution of the fluorescence of the divalent configuration is very small.

An additional, small component that we took into account in the fitting is the feature originating from quadrupolar transitions of Sm^{3+} . RXES can separate decay events that follow dipolar $2p \rightarrow 5d(E1)$ and quadrupolar $2p \rightarrow 4f(E2)$ excitation channels because they resonate at different $h\nu_{IN}$ and involve different energy transfers. The quadrupolar component is observed around $E_T = 1071$ eV in all Sm RXES spectra at 18 GPa excited from 6702 to 6706 eV (arrow in the main panel of Fig. 2) and resonates at $h\nu_{IN} = 6705$ eV. At lower pressures the quadrupolar feature A is too weak to be detected, also because it is superimposed to the fluorescence Sm^{2+} component. The assignment of feature A to the $E2$ transition of Sm^{3+} is supported by previous RXES experimental findings and calculations. In Refs. 19–21, the RXES spectra of Sm show two families of quadrupolar features that resonate at two different energies. One of them is feature A, and the other is expected to occur at energy transfer $E_T = 1068$ eV; i.e., around the energy transfer position of Sm^{2+} . In our analysis we modeled the presence of Sm^{3+} quadrupolar features through two shifted Gaussians, centered at ~ 1071 eV and at ~ 1068 eV and with linewidth ~ 3 eV. The relative intensity of two quadrupolar profiles is set equal to the value found in Ref. 20. An example of decomposition is given in the lower panel of Fig. 2: the dots represent the measured spectrum, the peak centered around 1077 eV is the trivalent component (decomposed in the two Gaussians that we used to model it), the $E2$ feature is the gray shaded area, made up of its two subcomponents (also shown). The residual, almost vanishing contribution at the lowest energy transfer side of the spectrum is the divalent component. The $E2$ excitation channel in Sm^{2+} was not observed in our data because the incident energy does not span a wide enough range below threshold.

The valencies extracted through the described procedure are displayed in Fig. 3. Two sets of valence values are reported, obtained from RXES spectra by including (open circles) or neglecting (filled circles) the quadrupolar component in the analysis. In the latter case the whole intensity in the low energy transfer region was attributed to the divalent component. Comparison of the two sets of data shows that the estimate of the valence change is affected only marginally by the exact modeling of the quadrupolar component, especially at high applied pressures, and gives an indication of the error bar, which amounts to $\sim 2-3\%$. In Fig. 3 we also reported the valence of Sm up to 7 GPa from the L_3 XAS results of Ref. 6. Good agreement with our values is observed. The precise evaluation of the valence values towards the completion of the transition to the trivalent state would have been very difficult by L_3 XAS due to the large uncertainties in the decomposition of spectra affected by the long lifetime of the $2p_{3/2}$ core-holes.

From the pressure dependence of the valence estimated from our Sm L_3 RXES results, the fully trivalent state is reached for pressures of the order of $p_c = 13$ GPa. Above this

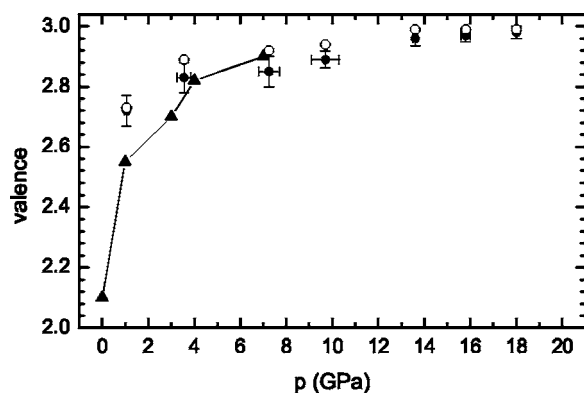


FIG. 3. Sm valence in SmS as a function of the applied pressure, obtained from the analysis of RXES spectra as described in the text, by including (open circles) or neglecting (filled circles) the quadrupolar component in the analysis. Filled triangles: previous Sm valence trend versus pressure up to 7.2 GPa determined from Sm L_{3} XAS (see Ref. 6).

pressure, a valence of 2.99(1), independent from pressure, is obtained when the quadrupolar transition is correctly taken into account. Although valence is a function of both pressure and temperature in intermediate valence systems, we do not expect in the case of SmS a strong variation in valence dependence upon pressure at low temperature.^{22,23} In fact, a comparison of our RXES with low temperature XAS data²⁴ indicates the same valence dependence upon pressure at all temperatures between 4.5 and 300 K up to 3 GPa, associated with a negligible thermal variation. We therefore expect that this direct determination of p_c has important implications on

the interpretation of the phase transitions observed previously at 2 GPa.^{10,12} First of all, it confirms that the onset of long-range magnetic order is not associated with the entrance into the trivalent state, but it occurs at a valence $v \approx 2.8$,⁹ as it was also observed in x-ray absorption data²⁴ in the magnetically ordered phase at 2.9 GPa and 4.5 K. On the other hand, the hyperfine interactions at the ^{149}Sm nuclei as determined in Ref. 10 do not show any anomaly around $p_c = 13$ GPa, but they have the expected values for a trivalent state already at 2 GPa and they show little change up to 19 GPa. The important consequence of this finding is therefore that the Sm $4f$ wave function is renormalized to an effective trivalent state (i.e., Sm behaves magnetically like a completely trivalent ion) well before the pressure p_c for the transition to the pure trivalent state is reached.

In conclusion, we have investigated the valence of Sm in SmS by resonant x-ray emission, in a wider pressure range than explored in previous experiments. In contrast to XAS, RXES is sensitive to even very small components of a given electronic configuration. The analysis of the Sm line shapes clearly shows that Sm becomes trivalent ($v \sim 2.99$) at $p_c \sim 13$ GPa. The implications of this result on the understanding of the onset of long-range magnetic order at 2 GPa call for more systematic studies of the correlations between valence and magnetic phase transitions in the compounds of anomalous lanthanides (especially in the cases of Ce and Yb).

The authors wish to thank S. Huotari, D. Braithwaite, and P. P. Deen for their support in the initial phase of the experiment.

*Now at IPCMS/GEMME, 23 rue du Loess-B.P. 43, F-67034 Strasbourg Cedex 2, France.

¹P. Wachter, in *Handbook on the Physics and Chemistry of Rare Earths*, edited by K. A. Gschneidner *et al.* (North-Holland, Amsterdam, 1994), Vol. 19, p. 383.

²A. Jayaraman, V. Narayanamurti, E. Bucher, and R. G. Maines, *Phys. Rev. Lett.* **25**, 1430 (1970).

³M. B. Maple and D. Wohlleben, *Phys. Rev. Lett.* **27**, 511 (1976).

⁴S. Raymond, J. P. Rueff, M. D'Astuto, D. Braithwaite, M. Krisch, and J. Flouquet, *Phys. Rev. B* **66**, 220301(R) (2002).

⁵F. Lapierre, M. Ribault, F. Holtzberg, and J. Flouquet, *Solid State Commun.* **40**, 347 (1981).

⁶J. Röhler, G. Krill, J.-P. Kappler, M. F. Ravet, and D. Wohlleben, in *Valence Instabilities*, edited by P. Wachter and H. Boppert (North-Holland, Amsterdam, 1982), p. 215.

⁷J. M. D. Coey, S. K. Ghatak, M. Avignon, and F. Holtzberg, *Phys. Rev. B* **14**, 3744 (1976).

⁸R. Keller, G. Güntherodt, W. B. Holzapfel, M. Dietrich, and F. Holtzberg, *Solid State Commun.* **29**, 753 (1979).

⁹V. N. Antonov, B. N. Harmon, and A. N. Yaresko, *Phys. Rev. B* **66**, 165208 (2002).

¹⁰A. Barla *et al.*, *Phys. Rev. Lett.* **92**, 066401 (2004).

¹¹A. Barla *et al.*, *J. Phys.: Condens. Matter* **17**, S837 (2005).

¹²Y. Haga *et al.*, *Phys. Rev. B* **70**, 220406(R) (2004).

¹³C. Dallera *et al.*, *Phys. Rev. B* **68**, 245114 (2003).

¹⁴C. Dallera, M. Grioni, A. Shukla, G. Vankó, J. L. Sarrao, J. P.

Rueff, and D. L. Cox, *Phys. Rev. Lett.* **88**, 196403 (2002).

¹⁵C. Dallera, E. Annese, J. P. Rueff, M. Grioni, G. Vankó, L. Braicovich, A. Barla, J. P. Sanchez, R. Gusmeroli, A. Palenzona, L. Degiorgi, and G. Lapertot, *J. Phys.: Condens. Matter* **17**, S849 (2005).

¹⁶E. Annese, J. P. Rueff, G. Vankó, M. Grioni, L. Braicovich, L. Degiorgi, R. Gusmeroli, and C. Dallera, *Phys. Rev. B* **70**, 075117 (2004).

¹⁷A. Kotani and S. Shin, *Rev. Mod. Phys.* **73**, 203 (2001).

¹⁸B. T. Thole, G. van der Laan, J. C. Fuggle, G. A. Sawatzky, R. C. Karnatak, and J.-M. Esteve, *Phys. Rev. B* **32**, 5107 (1985).

¹⁹F. Bartolomé, M. H. Krisch, D. Raoux, and J.-M. Tonnerre, *Phys. Rev. B* **60**, 13497 (1999).

²⁰F. Bartolomé, J.-M. Tonnerre, L. Sève, D. Raoux, J. Chaboy, L. M. Garcia, M. Krisch, and C. C. Kao, *Phys. Rev. Lett.* **79**, 3775 (1997).

²¹J.-J. Gallet, J.-M. Mariot, L. Journel, C. F. Hague, A. Rogalev, H. Ogasawara, A. Kotani, and M. Sacchi, *Phys. Rev. B* **60**, 14128 (1999).

²²I. Nowik, *Hyperfine Interact.* **13**, 89 (1983).

²³J. M. Tarascon, Y. Isikawa, B. Chevalier, J. Etourneau, P. Hagenmuller, and M. Kasaya, *J. Phys. (France)* **41**, 1141 (1980).

²⁴P. P. Deen, D. Braithwaite, N. Kernavanois, L. Paolasini, S. Raymond, A. Barla, G. Lapertot, and J. P. Sanchez, *Phys. Rev. B* **71**, 245118 (2005).